

Innovative remote sensing methodologies and applications in coastal and marine environments

Qing Zhao, Antonio Pepe, Virginia Zamparelli, Pietro Mastro, Francesco Falabella, Saygin Abdikan, Caglar Bayik, Fusun Balik Sanli, Mustafa Ustuner, Nevin Betul Avşar, Jingjing Wang, Peng Chen, Zhengjie Li, Adam T. Devlin & Fabiana Calò

To cite this article: Qing Zhao, Antonio Pepe, Virginia Zamparelli, Pietro Mastro, Francesco Falabella, Saygin Abdikan, Caglar Bayik, Fusun Balik Sanli, Mustafa Ustuner, Nevin Betul Avşar, Jingjing Wang, Peng Chen, Zhengjie Li, Adam T. Devlin & Fabiana Calò (2024) Innovative remote sensing methodologies and applications in coastal and marine environments, *Geo-spatial Information Science*, 27:3, 836-853, DOI: [10.1080/10095020.2023.2244006](https://doi.org/10.1080/10095020.2023.2244006)

To link to this article: <https://doi.org/10.1080/10095020.2023.2244006>



© 2023 Wuhan University. Published by Informa UK Limited, trading as Taylor & Francis Group.



Published online: 06 Sep 2023.



[Submit your article to this journal](#)



Article views: 2624



[View related articles](#)



[View Crossmark data](#)



Citing articles: 8 [View citing articles](#)

Innovative remote sensing methodologies and applications in coastal and marine environments

Qing Zhao ^{a,b,c}, Antonio Pepe ^{d,e}, Virginia Zamparelli ^d, Pietro Mastro ^d, Francesco Falabella ^{d,f}, Saygin Abdikan ^g, Caglar Bayik ^h, Fusun Balik Sanli ⁱ, Mustafa Ustuner ^j, Nevin Betul Avşar ^k, Jingjing Wang ^{a,b,c}, Peng Chen ^{a,b,c}, Zhengjie Li ^{a,b,c}, Adam T. Devlin ^l and Fabiana Calò ^d

^aKey Laboratory of Geographical Information Science, Ministry of Education, East China Normal University, Shanghai, China; ^bSchool of Geographic Sciences, East China Normal University, Shanghai, China; ^cKey Laboratory of Spatial-Temporal Big Data Analysis and Application of Natural Resources in Megacities, Ministry of Natural Resources, Shanghai, China; ^dInstitute for Electromagnetic Sensing of the Environment (IREA), Italian National Research Council, Napoli, Italy; ^eSchool of Engineering, University of Basilicata, Potenza, Italy; ^fInstitute of Methodologies for Environmental Analysis (IMAA), Italian National Research Council, Tito Scalo, Italy; ^gDepartment of Geomatics Engineering, Hacettepe University, Ankara, Turkey; ^hDepartment of Geomatics Engineering, Zonguldak Bulent Ecevit University, Zonguldak, Turkey; ⁱDepartment of Geomatic Engineering, Yildiz Technical University, Istanbul, Turkey; ^jDepartment of Geomatic Engineering, Artvin Çoruh University, Artvin, Turkey; ^kDepartment of Geomatics Engineering, Izmir Katip Celebi University, Izmir, Turkey; ^lSchool of Ocean and Earth Science and Technology, University of Hawaii at Mānoa, Honolulu, HI, USA

ABSTRACT

Remote sensing (RS) technologies are extensively exploited by scientists and a vast audience of local authorities, urban managers, and city planners. Coastal regions, geohazard-prone areas, and highly populated cities represent natural laboratories to apply RS technologies and test new methods. Over the last decades, many efforts have been spent on improving Earth's surface monitoring, including intensifying Earth Observation (EO) operations by the major national space agencies. They oversee to plan and make operational constellations of satellite sensors providing the scientific community with extensive research and development opportunities in the geoscience field. For instance, within this framework, the European Space Agency (ESA) and the Ministry of Science and Technology of China (MOST) have sponsored, since the early 2000s, the DRAGON initiative jointly carried out by the European and Chinese RS scientific communities. This manuscript aims to provide a synthetic overview of some research activities and new methods recently designed and applied and trace the route for further developments. The main findings are related to i) the analysis of flood risk in China, ii) the potential of new methods for the estimation and removal of ground displacement biases in small-baseline oriented interferometric Synthetic Aperture Radar (SAR) methods, iii) the analysis of the inundation risk in low-lying regions using coherent and incoherent SAR methods; and iv) the use of SAR-based technologies for marine applications.

ARTICLE HISTORY

Received 30 January 2023
Accepted 31 July 2023

KEYWORDS

Disaster risk management; Remote Sensing (RS); Earth Observation (EO); Synthetic Aperture Radar (SAR); flooding; subsidence; coastal/marine environments

1. Introduction

Coastal areas are particularly exposed to a combination of risk factors, such as extreme weather events, climate change effects and sea level rise, resulting in the world's most vulnerable regions. In these areas, often highly populated, many key civil sectors, e.g. public/private infrastructures, cultural/natural heritage and agriculture, are heavily affected by natural and man-made hazards (Calò et al. 2015), with severe socio-economic consequences. In such fragile environments, Remote Sensing (RS) technologies may be profitably exploited to detect and monitor changes in Earth's surface systematically, efficiently and with reduced costs. Several studies showing the power of RS data and methods for studying and protecting coastal and river delta regions worldwide are present in the scientific literature, for instance, see the works (Klemas 2015; Kratzer et al.

2016; Laignel et al. 2023; Zhao et al. 2022) and references therein. Microwave sensors are also becoming valuable tools for understanding marine phenomena affecting the sea surface (Kerbaol and Collard 2005) and inland water (Amadori et al. 2021).

The interest in such topics has motivated the European Space Agency (ESA) and the Ministry of Science and Technology of China (MOST) to foster the development of joint initiatives and fund the DRAGON Cooperation Program as an opportunity for European and Chinese scientists and stakeholders to cross-fertilize their expertise and valorize their inherent space mission technologies.

In this work, the participants in the DRAGON 5 project entitled "Global climate change, sea level Rise, Extreme Events and local ground subsidence effects in

CONTACT Antonio Pepe  pepe.a@irea.cnr.it

Coastal and river delta regions through Novel and Integrated remote sensing approaches” (GREENISH) («Global Climate Change 2023, Sea Level Rise, Extreme Events and Local Ground Subsidence Effects in Coastal and River Delta Regions through Novel and Integrated Remote Sensing Approaches (GREENISH)» s.d.) will provide readers with an analysis of conventional and innovative RS methodologies used within the project, and related applications in different test sites, showing the capability of these technologies for the investigation of coastal and marine environments.

The manuscript is organized as follows. Section 2 summarizes the used RS methods and shortly provides technical details. Section 3 shows the results of the analyses carried out within four primary research activities. More specifically, Section 3.1 focuses on the research performed in several test sites in China, including the study of flooding impact on the coastal area of Shanghai. Section 3.2 is devoted to interferometric Synthetic Aperture Radar (SAR) technology advancements; mainly, we investigate the capability of a recently developed method (Falabella and Pepe 2022a) for estimating and compensating ground displacement biases in Sentinel-1 interferograms, with applications in case studies in Italy and U.S. The results of the SAR- and AI-based analyses related to flooding risk are shown in Section 3.3, focusing on the Venice lagoon area, Italy. Section 3.4 provides insights into the potential of SAR-based techniques for marine environment investigation. Discussion and concluding remarks are finally addressed in Sections 4 and 5.

2. Data and methods

2.1. Satellite SAR datasets

Several image datasets acquired by different SAR satellite sensors have been exploited for the research experiments performed over the investigated areas. Table 1 summarizes the information about the data used for every site.

2.2. Conventional and novel SAR technologies

This section is focused on the EO SAR technologies mainly exploited in this work, shortly providing information on their rationale and application fields. One of the most successful SAR-based applications is the detection and monitoring of ground movements by processing multi-temporal images through Mt-InSAR methods (Berardino et al. 2002; Ferretti et al. 2011; Ferretti, Prati, and Rocca 2001; Pepe and Lanari 2006; Pepe et al. 2015). Among these, the Small Baseline Subset (SBAS) approach (Berardino et al. 2002) proved very attractive for detecting displacements of distributed targets in heterogeneous land cover areas. It relies on the computation of a sequence of multi-looked SAR interferograms with small perpendicular baselines to reduce the impact of decorrelation noise artifacts on the deformation measurements (Berardino et al. 2002; Pepe et al. 2015). For every analyzed SAR pixel, a system of linear equations that relate the ground deformations of single interferometric SAR data pairs to those of the available time series of acquisitions is solved in the Least-Squares (LS) sense by linking independent sets of non-fully-connected SAR acquisitions using the singular value decomposition method (Hooper 2008; Pepe 2021; Pepe et al. 2015).

Within this context, recently, some problems have been highlighted. In particular, a lack of consistency that exists among triplets of multi-look SAR interferograms while ground displacement time-series are generated through Small Baseline (SB) InSAR algorithms (Berardino et al. 2002; Pepe and Lanari 2006) have been revealed in Falabella and Pepe (2022b). Indeed, unlike the random nature of phase triplets, some scholars have recently demonstrated that phase triplets can be related to systematic physical sources, such as soil moisture and/or other localized signals that lead to contributions in multi-looked SAR interferograms. In particular, it has been proven that a systematic phase bias is a short-living signal that evolves over short periods (Ansari, De Zan, and Parizzi 2021). Different methods have been proposed to estimate and compensate for such spurious signals

Table 1. SAR datasets and digital elevation models used for the presented investigations.

Study areas	SAR dataset	Acquisition Time	Scope/Application
Coastal Sites in China (Section 3.1)	SRTM DEM	2000	Analysis of flooding impact on coastal regions
	Tandem-X DEM	2015	
	RADARSAT-2 Multi-Look Fine		
	RADARSAT-2 Wide	2007–2017	
Nevada (USA)	Sentinel-1A	2018–2021	Assessment of multi-temporal InSAR time-series precision
	Sentinel-1A	2020–2021	
Southern Italy (Section 3.2)		2014–2022	
Venice Lagoon, Italy (Section 3.3)	Sentinel-1A	2017–2021	Analysis of subsidence and land changes detection in areas prone to flood risk
Mediterranean Sea region (Section 3.4)	ENVISAT ASAR	September 2010	Sea current analysis in marine environments

in the generated time series of ground displacements over the last 2 years (Falabella and Pepe 2022b; Maghsoudi et al. 2022; Zheng et al. 2022). Expressly, here we point out the method proposed in Falabella and Pepe (2022b) that benefits from the knowledge of phase non-closure signal properties among sets of time-redundant networks of interferograms. Considering a local (concerning time) approximation of a speckle noise model for multi-looked interferograms, it permits us to approximate the (unknown) systematic phase bias signal related to a generic interferogram computed from a couple of SAR images acquired at times t_h and t_k as follows:

$$\Delta\phi_{h,k}^{bias}(t_h - t_k) \cong [v + \Delta v(t_h - t_k)](t_h - t_k) \quad (1)$$

Using Equation (1) and assuming that the adopted model is time-invariant (i.e. the phase bias depends exclusively on the temporal baseline of the considered interferogram), and after simple mathematical manipulations, the generic phase triplet relevant to the three SAR images collected at times t_h , t_k and t_q , respectively, see Figure 1, can be expressed as:

$$\begin{aligned} \Delta\phi_{h,k,q}^{bias} \cong W_r [\Delta v(\Delta t_{h,k}) \Delta t_{h,k} + \Delta v(\Delta t_{k,q}) \\ \Delta t_{k,q} + \Delta v(\Delta t_{q,h}) \Delta t_{q,h}] \end{aligned} \quad (2)$$

Note that the temporal baseline of SAR interferograms is necessarily a quantized value proportional to the atomic repetition time of the considered constellation of SAR sensors. For instance, when Sentinel-1A/B SAR data are considered, in the twin mode, the value of δ is equal to 6 days. Then, Equation 2 leads to the formulation of the following system of linear equations:

$$Z \cdot \Delta V = \Delta\phi_{tr}^{bias} \quad (3)$$

where Z is the incidence-like matrix of the involved linear transformation from the N acceleration values $\Delta V = [\Delta v(\delta), \Delta v(2\delta), \dots, \Delta v(N\delta)]^T$ of the systematic

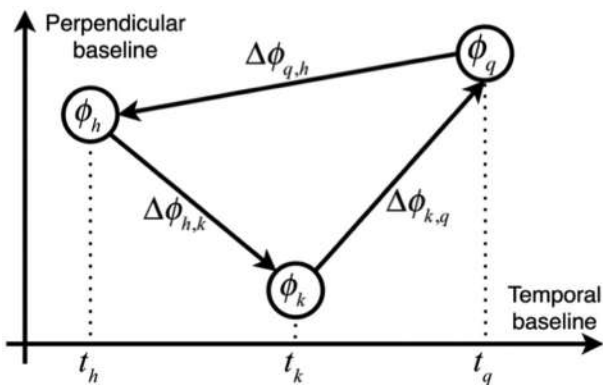


Figure 1. Pictorial representation of a generic phase triplet consisting of three multi-looked InSAR phases in the perpendicular/temporal baseline plane. The three interferograms are formed from three SAR acquisitions, acquired at different time instants.

phase-biased vector and the measured phase triplets $\Delta\phi_{tr}^{bias}$. The system (3) is hence solved in the LS sense; once obtained, the estimates of the phase acceleration terms at the different temporal baselines are used to compute the phase biases at different temporal baselines using the following iterative equation (Falabella and Pepe 2022b):

$$\begin{aligned} \Delta\phi^{bias}[\xi\delta] = \frac{\xi}{\xi + 1} \Delta\phi^{bias}[(\xi + 1)\delta] \\ + \xi\delta\{\Delta v(\xi\delta) - \Delta v[(\xi + 1)\delta]\} \end{aligned} \quad (4)$$

with the initial condition that the phase bias at the longest used temporal baseline (e.g. with values longer than 90–100 days) of the available SB dataset is almost zero. An enhanced version of the developed method, also considering the time-variant case, was also developed and detailed in Falabella and Pepe (2022b), where interested readers can find additional details on implementing the proposed phase bias compensation method and relevant experimental results with Sentinel-1 SAR data are shown.

Developing and applying coherent and incoherent approaches for land cover change detection nowadays represent another significant SAR research field. Although SAR images have been less exploited than optical data, microwave active sensors are very promising for Change Detection (CD) analyses (Barber 2015; Bazi, Bruzzone, and Melgani 2006; Mastro et al. 2022) since they work in all-weather and sunlight conditions. These peculiarities and the growing availability of free-of-charge data collected by several SAR constellations (e.g. the twin Sentinel-1A/B sensors) make SAR data use very attractive for CD applications.

In this work, CD methods have been complemented with the InSAR technique for flooding risk analyses, and the potential of a newly developed Artificial Intelligence (AI) method (Mastro et al. 2022) based on Random Forest (RF) (Belgiu and Drăguț 2016; Breiman 2001) has been exploited. This methodology leverages the capability of several coherent/incoherent SAR Change Detection Indices (CDIs) and their mutual interaction in a single corpus for rapid mapping of surface changes (Mastro et al. 2022). The results of such investigations are detailed in Mastro et al. (2022) and summarized in Section 3.3. Figure 2 describes the main steps of the developed interlinked approach that combines coherent and incoherent SAR descriptors for CD analyses.

The third main research topic addressed here is the use of SAR-based techniques for sea state monitoring, representing a supporting tool for coastal area protection. Over the last decade, the scientific community's interest in studying marine parameters exploiting SAR has increased. The use of SAR data for oil-spill monitoring (Fiscella et al. 2000; Trivero et al. 2016), ship and sea-ice detection (Tello, Lopez-Martinez, and

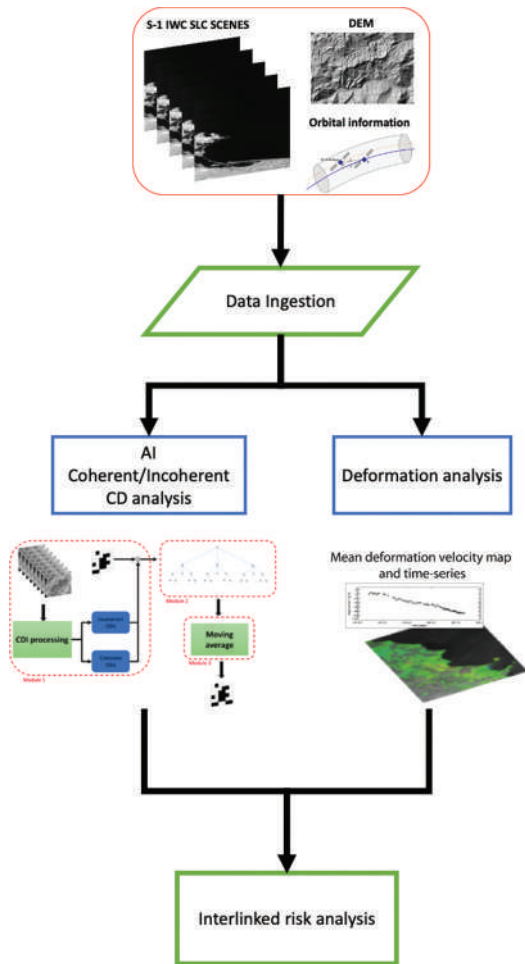


Figure 2. Interlinked risk analysis flowchart.

Mallorqui 2005; Zakhvatkina, Smirnov, and Bychkova 2019) is well established, and it is becoming more and more beneficial for understanding marine phenomena (Kerbaol and Collard 2005), complementing the traditional use of optical or multispectral images (Bresciani et al. 2021).

We estimate the sea surface current among the different marine phenomena by analyzing SAR data. The extraction of quantitative sea surface parameters relying only on SAR amplitude images is a rather complex matter. Many variables are involved in determining the backscatter, such as the wind vector, bathymetry, etc. For this reason, similarly to other SAR applications, phase information may provide valuable information.

Sea surface current velocity can be estimated using two different SAR data processing techniques: the Along-Track Interferometry (ATI) (Romeiser et al. 2014) and the Doppler Centroid Anomaly (DCA) method (Zamparelli et al. 2020). Both methods allow only to measure the radial component of the sea surface velocity, i.e. the component along the Line Of Sight (LOS) of the radar. ATI exploits SAR data pairs acquired with the same look-angle but with two slightly different acquisition times (Romeiser et al. 2014). Hence, this technique requires unique sensor

characteristics, i.e. the possibility of having two SAR antennas dislocated along the radar flight track (azimuth direction). This way, the radar signal related to the same target is collected by the different antennas within a short time lag. Accordingly, the targets' movements translate to phase shifts on the interferometric phase difference. The radial component of the sea surface currents can be achieved over broad areas starting from the use of the spectral analysis and specifically the estimation of the local DCA induced by the movement of the scattering mechanisms (Romeiser et al. 2014; Zamparelli et al. 2020). DCA uses a single SAR image based on spectral estimation. The goal is to measure the residual Doppler shifts of the radar echoes by analyzing the distribution of the azimuth Power Spectral Density (PSD) (Madsen 1989). DCA is obtained by subtracting from the Doppler Centroid the term corresponding to a "stationary" scene, e.g. the set where all scatterers move at the same velocity associated with the Earth rotation (Zamparelli et al. 2020); see Figure 3.

More specifically, given a target moving with a radial velocity v_r , the Doppler Centroid Anomaly f_{DCA} can be estimated to derive v_r :

$$f_{DCA}(x, r) = f_{DC}(x, r) - f_{DC0}(x, r) = \frac{2}{\lambda} v_r(x, r) \quad (5)$$

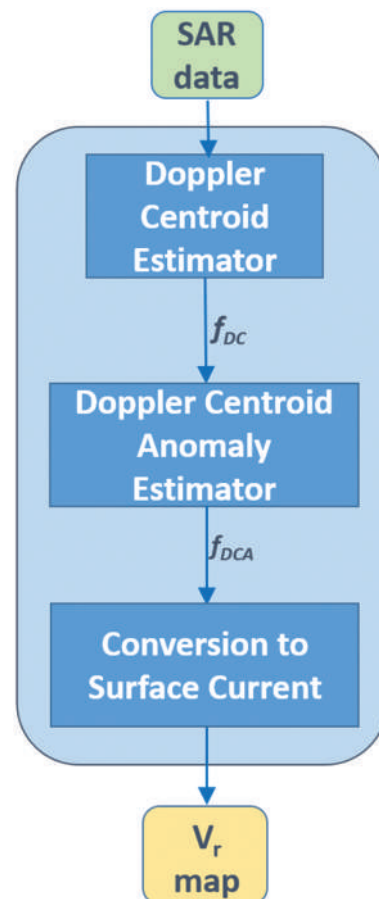


Figure 3. Block diagram of the DCA method.

where x and r are the azimuth and range, respectively, f_{DC} is the Doppler Centroid (DC) measured from the data, f_{DC0} is the DC corresponding to the stationary scene, λ is the sensor wavelength. Hence, the surface radial velocity v_r , i.e. the component along the LOS, can finally be estimated from the DCA described in Equation (5) as follows:

$$v_r = \frac{\lambda}{2} f_{DCA} \quad (6)$$

The described technique has often been applied in the literature, and typically it is referred to oceanic regions (Johannessen et al. 2008), characterized by intensive water mass movement. This characteristic allows easily separating, from a qualitative point of view, components associated with ocean dynamics from meteorological inferred sources.

Conversely, the Mediterranean Sea is characterized by currents ranging in a much-limited interval compared to the ocean case. Examples of sea surface current extraction can be found in the works (Cianelli et al. 2012; Zamparelli et al. 2020).

3. Experimental results

3.1. Analyses of coastal regions in China

SAR-based investigations have been carried out over selected areas in China (Figure 4). First, the terrain elevation changes of newly reclaimed lands of some Chinese coastal cities (i.e. Dalian, Ningbo, Tangshan, Yancheng, Nantong and Tianjin) have been derived by

simply comparing the differences of digital elevation models available for the studied areas, computed by the Shuttle Radar Topography Mission (SRTM) in 2000 (Rosen et al. 2001), and the Tandem-X (Romeiser et al. 2014) mission in 2015. Figure 4 shows the geographical location of the identified areas of interest, where Figure 5 show the spatial distribution of new lands reclaimed from 2000 to 2015. Reclaimed land projects also characterize the coastal area of the Shanghai megacity, where further analyses have been conducted. Several investigations (Bates and De Roo 2000; Pepe and Calò 2017; Pepe et al. 2016; Tang et al. 2022) have been carried out in recent years to track changes and detect ground displacements in the Shanghai district. The relevant results have been beneficial in studying the coastal erosion, inundation, and sea-level-rise phenomena. For instance, the LISFLOOD-FP hydrodynamic model (Qin, Wu, and Xiu 2019) was employed to map coastal inundation areas along the eastern coast of Shanghai. The results demonstrated that over 80% of the flooded regions are newly reclaimed lands. The model describes the dynamic propagation of waves on floodplains using continuity and momentum equations, discretized over a grid mesh (Kennish et al. 2010; Teatini et al. 2005). Three kinds of information are used to run the model: i) a digital elevation model describing the height topography of the coastal area, ii) the sea-water depth as derived from the Global Tide and Surge Reanalysis (GTSR), iii) a set of boundary conditions describing the initial state of flood along the coast. Seawalls height and the coastal ground

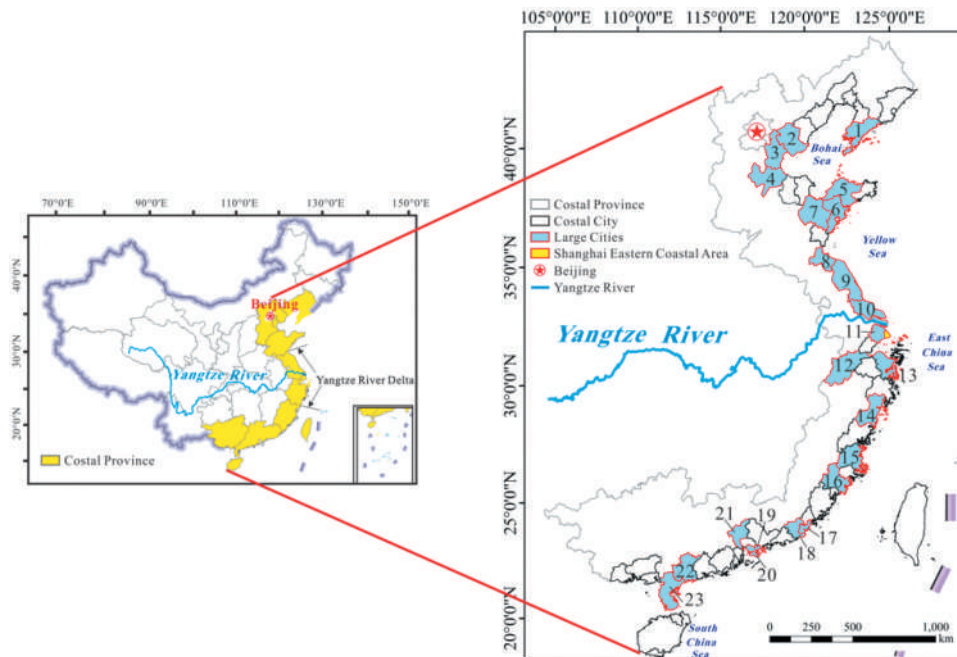


Figure 4. A map of locations of the large cities on the coast of mainland China investigated in the work (Tang et al. 2022): (1) Dalian; (2) Tangshan; (3) Tianjin; (4) Cangzhou; (5) Yantai; (6) Qingdao; (7) Weifang; (8) Lianyungang; (9) Yancheng; (10) Nantong; (11) Shanghai; (12) Hangzhou; (13) Ningbo; (14) Wenzhou; (15) Fuzhou; (16) Quanzhou; (17) Shantou; (18) Jieyang; (19) Shenzhen; (20) Hong Kong; (21) Guangzhou; (22) Maoming; and (23) Zhanjiang.

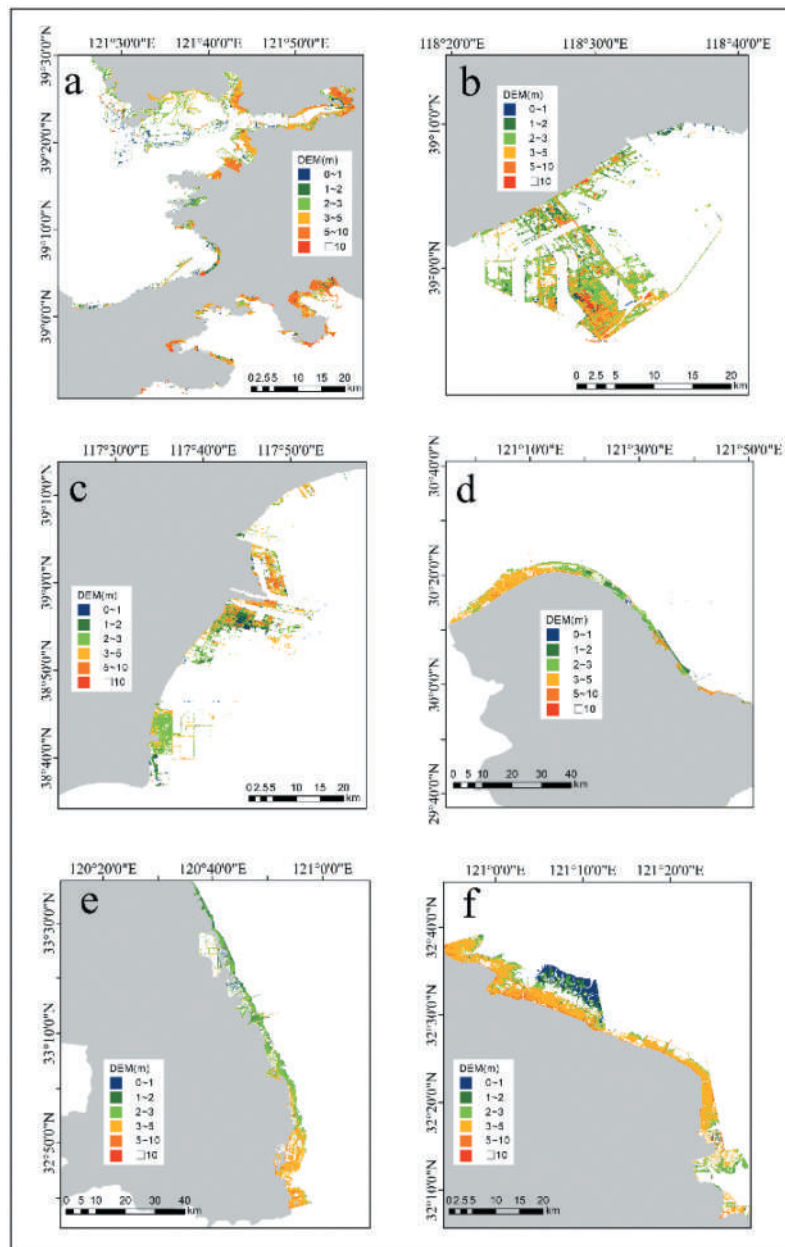


Figure 5. The terrain elevation changes of newly reclaimed land in selected coastal areas, i.e. (a) Dalian, (b) Tangshan, (c) Tianjin, (d) Ningbo, (e) Yancheng, (f) Nantong, obtained by comparing SRTM DEM (2000) and TanDEM-X (2015) (Tang et al. 2022).

displacements (e.g. the up-down deformations) were jointly used to constrain the solution (i.e. the extent and height of flooded water column) to consider the presence along the coast of seawalls for safeguarding and the subsidence which can increase the inundation risk (Qin, Wu, and Xiu 2019). The ground displacement time series of Shanghai and its coastal region, spanning the time interval between 2018 and 2021, were derived by applying the SBAS technique (Berardino et al. 2002; Pepe and Lanari 2006) to two independent sets of SAR images collected by the X-band COSMO-SkyMed (CSK) (descending orbits) and the C-band European Copernicus Sentinel-1 (S-1) (ascending orbits) sensors. The east-west and up-down deformation time series, calculated for every coherent point common to both SAR datasets, were

retrieved using the minimum acceleration multi-track InSAR method (Pepe et al. 2016; Shirzaei 2015). To study the flooding risk over the selected area, we performed several simulations using the LISFLOOD-FP mentioned above model. In particular, the coastline seawalls of the eastern Shanghai area were divided into the 40 segments shown in Figure 6(a). For every segment, we computed a distinctive simulation running the LISFLOOD-FP model. In case of an extreme weather event, we assumed that a specific seawall segment could fail and be destroyed, leading waves to overtop the barriers and flood the nearby lands. Moreover, we also observed that the southern coastline segments of the Pudong district of Shanghai are characterized by lower seawall heights and high ground deformation rates; accordingly, they have the

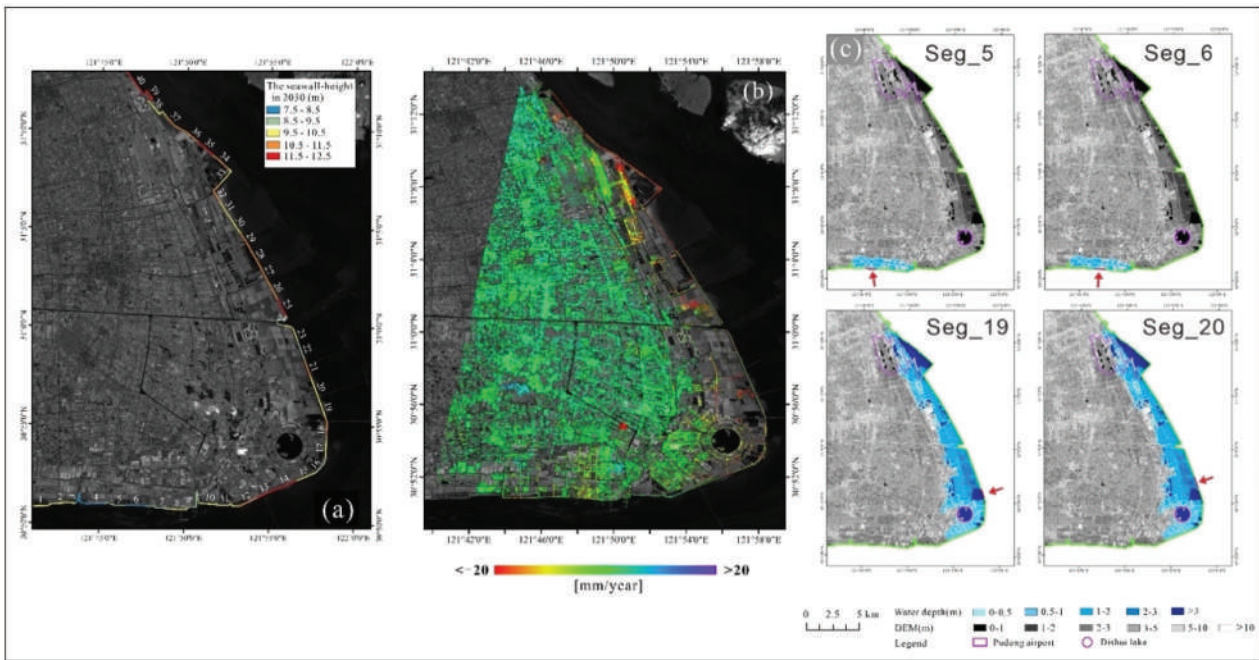


Figure 6. (A) Seawall heights for the selected 40 segments in Shanghai; (b) Map of 2018–2021 geocoded mean deformation velocity along the up–down direction; (c) Four simulated inundation scenarios with a 100-year return period flood. The red arrows indicate where the wave is assumed to overtop (Tang et al. 2022).

highest probability of wave overtopping. At the same time, we noted that the number of infrastructures potentially subjected to severe flood impacts in the southern sector of the coast is more significant than in other sectors (Tang et al. 2022). presented a detailed analysis on these experiments. The inundation extents and depths under the failure scenarios of different sections of the seawalls and 100-year return period flood were simulated and mapped. The simulations (as earlier said) take account of the coastal ground subsidence as derived from InSAR analyses. Figure 6(b) shows the geocoded map of the mean deformation velocity of the eastern Shanghai zone in the up–down direction from 2018 to 2021. Figure 6(c) shows the inundation extents and depths under the failure scenarios of seawall sectors 5–6 and 19–20. The inundation depths are divided into five levels represented by different brightness values on a blue scale. As shown in Figure 6(c), after the failure of the seawall in sectors 19–20, the eastern coastal areas (including a part of Pudong International Airport) would be flooded. While after the failure of the seawall in sectors 5–6, the inundation areas were minimal. The impact in terms of coherent structures potentially damaged by the inundation was further quantified in the work (Tang et al. 2022).

$\Delta V = [\Delta v(\delta), \Delta v(2\delta), \dots, \Delta v(N\delta)]^T$ Finally, the analysis of the land use – land cover changes due to the heavy urbanization of the region has been carried out. We employed three deep learning models, including U-Net, U^2 -Net, and Res-UNet (Qin, Wu, and Xiu 2019), to detect urban building change in Shanghai.

Ten TSX images acquired in StripMap mode from 16 October 2015 to 19 August 2016 were used in this study. Before training these networks, we pre-processed TSX images and generated ten TSX Backscatter Intensity Maps (BIMs) and nine Coherence Maps (CMs), fed into the network models. The BIMs were obtained by conducting multi-looking on each Single-Look-Complex (SLC) image with the ratio of range and azimuth (2:3). CMs were derived by performing interferometry on two SLC images with adjacent acquisition time and computing the coherence values of interferograms. The spatial resolution of BIMs and CMs is $6\text{ m} \times 6\text{ m}$. We divided the BIMs and CMs into small non-overlapping patches of 512×512 pixels, forming three training samples and one test sample (see Figure 7 for location). Then, the training samples were employed to obtain the weight parameters of three models, and the test sample was utilized for verifying urban building change detection accuracy. The results show that the deep learning models and high-resolution SAR image information can be used for obtaining reliable urban change results (see Figure 8).

The urban change detection maps derived from three deep learning models and TSX image information are illustrated in Figure 8(a). Res-UNet exhibits the best visual performance, with fewer missing/false detections when BIMs and CMs are input datasets. In contrast, some pixels are mistakenly detected in the results of U-Net and U^2 -Net. The quantitative assessment is listed in Figure 8(b). The reference change map shown in Figure 8(c) was derived by interpreting



Figure 7. Coverage of TerraSAR-X (TSX) images and locations of training and test samples.

the differences between two SPOT images acquired on 13 October 2015 and 26 July 2016, with a spatial resolution of 1.5 m. Res-UNet achieves the best results with the highest Precision (85.46%), Recall (80.55%), F1-Score (82.87%), and Accuracy (99.66%) when inputting BIMs and CMs data. Therefore, the results show that Res-UNet can extract multi-source features and performs better than other models.

3.2. Insights on the biased estimates of ground displacements with MT-InsAR SBAS method with applications in USA and Italy

We estimated the bias affecting the ground displacements computed with the SB MT-INSAR approach by exploiting S-1 images acquired over a test site in Nevada (USA) from January 2020 to January 2021. Figure 9 shows the effect of biased phase compensation.

Unfortunately, starting from December 2021, the Sentinel-1B sensor malfunctioned, and ESA recently announced a move-up to launch a replacement sensor. Accordingly, using SAR datasets also including 2022-year SAR acquisitions has an impact on the developed phase bias compensation method that might suffer in the correction of such systematic phase artifacts, especially with periods of 6 days, even though the algorithm is still capable of reducing the phase bias signals moving from different sets of SB interferograms. As a further experiment, we applied the summarized time-invariant and time-variant phase mitigation

methods (Falabella and Pepe 2022b) to a SAR dataset collected from 14 October 2014 to 13 November 2022, over a study area in southern Italy, consisting of 385 S-1 images (descending orbits). Figure 10(a) shows the mean ground displacement velocity of the area. Only SAR pixels correctly analyzed and characterized by temporal coherence values larger than 0.7 are portrayed in the map, where temporal coherence is a quality factor (Pepe and Mastro 2017; Pepe, Mastro, and Jones 2021), initially introduced in Pepe and Lanari (2006) and widely used in the reference literature, which quantifies synthetically the agreement between the generated displacement time-series and the used multi-look SAR interferograms (Falabella and Pepe 2022b; Pepe and Lanari 2006). Figure 10(b,c) shows the average mean ground displacement difference between time series obtained with SB networks with maximum temporal baselines of 6 and 148 days without (b) and with (c) the application of the developed phase bias compensation method, respectively.

To make the average improvement due to phase compensation evident, we plot in Figure 11 the average absolute mean biased ground displacement (concerning the reference SB network with a maximum temporal baseline of 148 days) considering the group of SAR pixels with temporal coherence values larger than 0.7. Red stars refer to the solution obtained with the described time-invariant method. In contrast, blue triangles refer to the time-variant case.

3.3. Interferometric SAR and change detection investigation

In this Section, we address the impacts of floods and extreme weather events on coastal region cultural heritage by focusing on the monumental city of Venice, Italy, and its lagoon area. The Venice Lagoon represents the most extensive lagoon system in Italy, one of the largest in the Mediterranean Sea, and one of the most strategic industrial areas in the country. The city of Venice represents a world-known extraordinary archeological, architectural, artistic, and cultural heritage masterpiece. The lagoon ecosystem (Kennish et al. 2010) is characterized by different drivers of change (land-based feeding activities, heavy metal extraction, ground-water extraction, etc.), causing multiple environmental impacts on the area (Teatini et al. 2005); the subsidence phenomenon of the terrain is one of the most important. Flooding events have always occurred in the Venice lagoon, mainly resulting from tides, seiches, and easterly winds; however, in the last decades, floods have become increasingly frequent due to the impact of climate changes on the sea level rise.

In such a context, RS analyses aimed at mapping and monitoring ground subsidence and flooding event were performed. Figure 12 shows

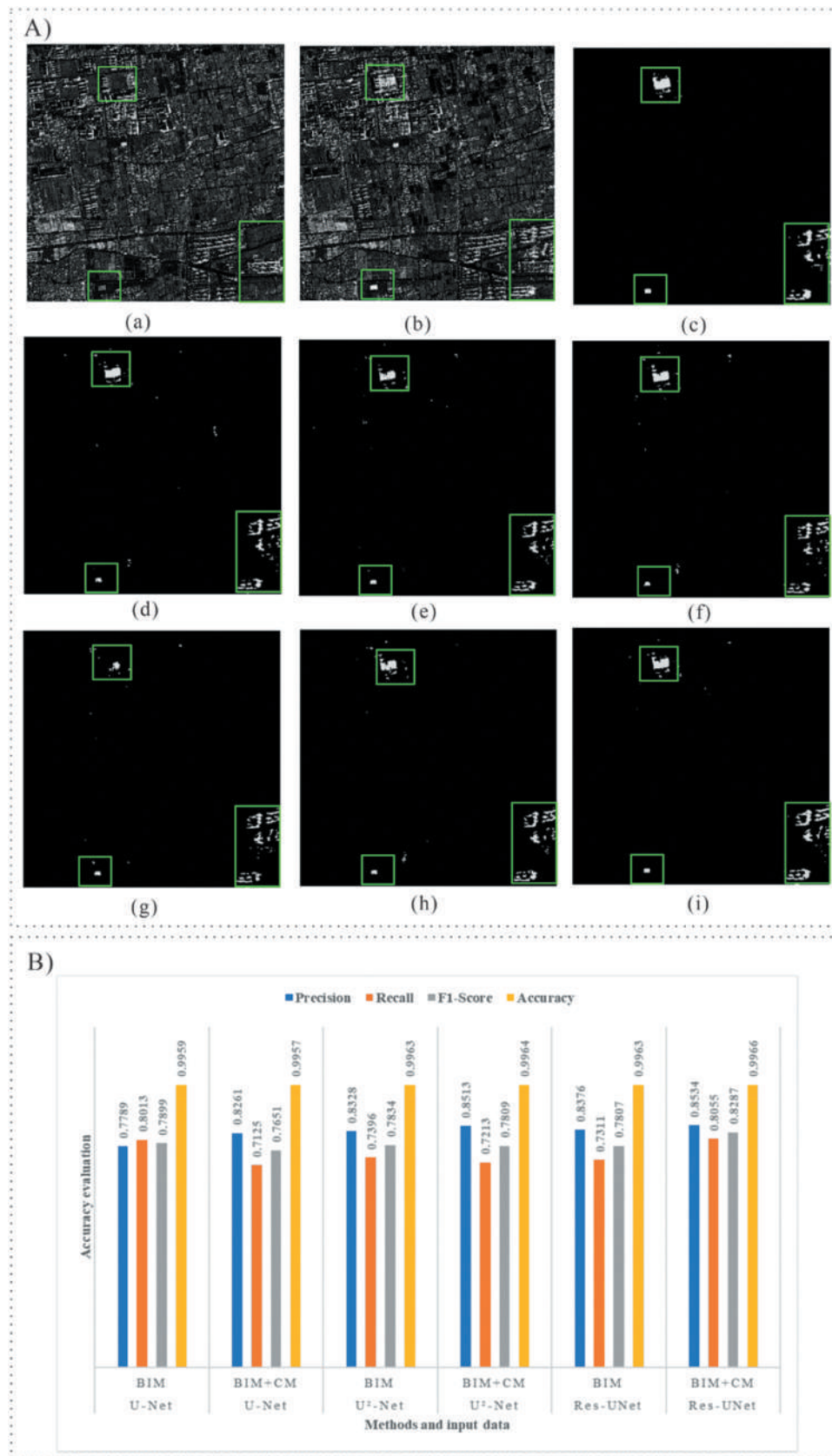


Figure 8. A) Urban change detection maps derived from three deep learning models and TSX image information. (a) and (b) are the images before and after the period where changes happened; (c) is the reference change map; (d), (e), and (f) represent the prediction results of U-Net, U²-Net, and Res-UNet, respectively, BIMs are input data; (g), (h), and (i) the prediction results of U-Net, U²-Net, and Res-UNet respectively, BIMs and CMs are input data. B) Comparisons of urban change detection results obtained by different models and input datasets.

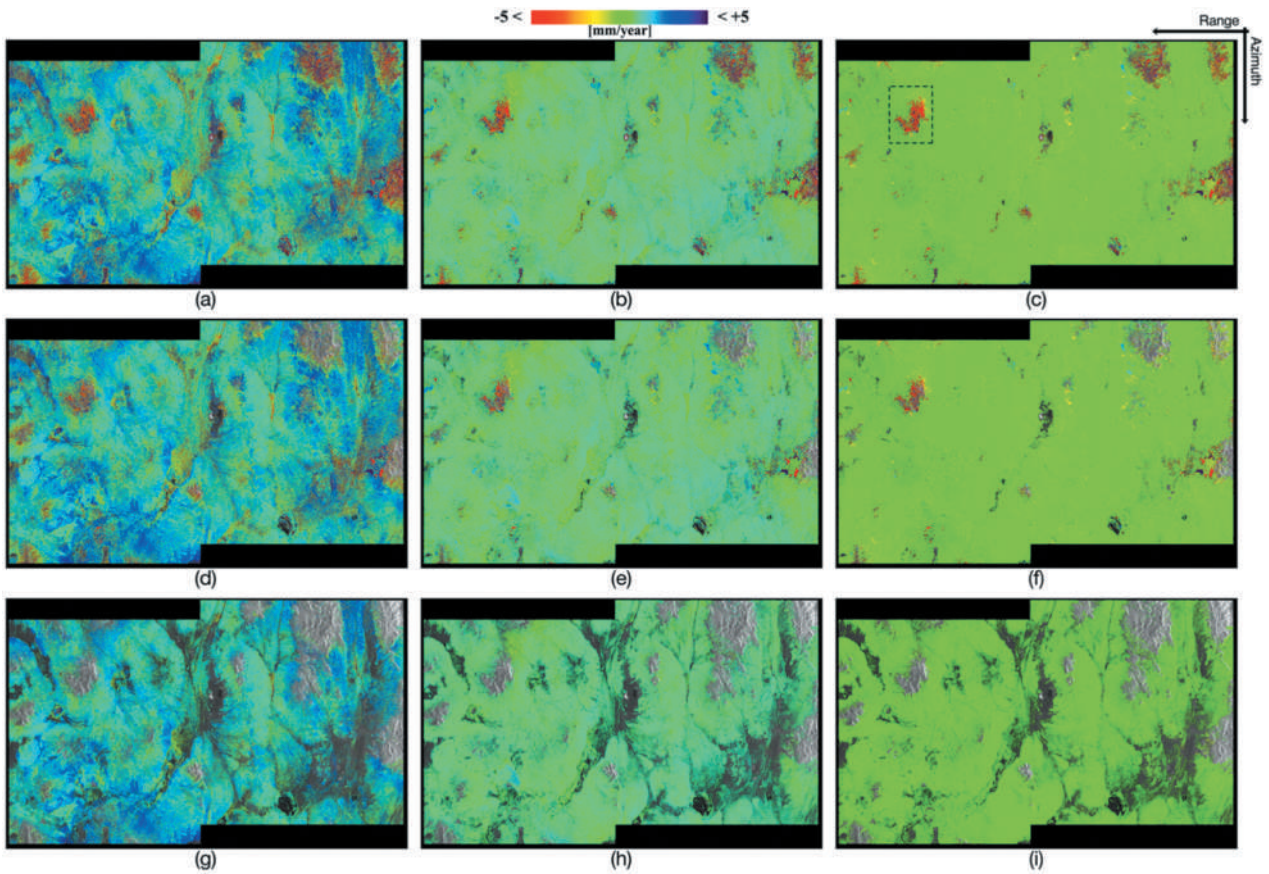


Figure 9. Nevada, USA: Maps of ground deformation velocity differences between the case at 12 and 96 days, where only pixels larger than given values of temporal coherence are depicted. (a), (d), (g) Bias considering the original interferograms. (b), (e), (h) Bias when the time-invariant correction method is applied. (c), (f), (i) Bias when applying the time-variant correction method. Temporal coherence greater than 0.7 (a)–(c), 0.9 (d)–(f), and 0.98 (g)–(i).

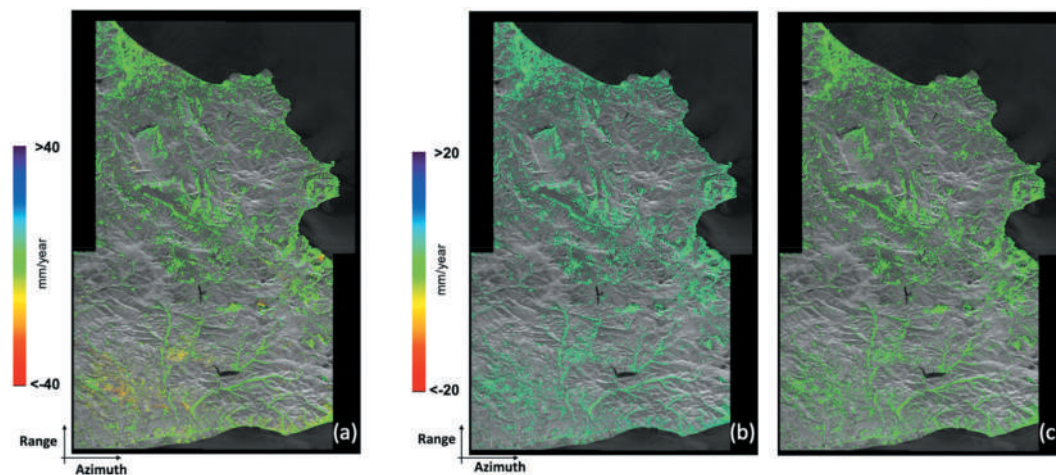


Figure 10. Experiments in Italy: (a) Mean displacement velocity map computed applying the SBAS method to a network of interferograms characterized by a maximum temporal baseline of 148 days. (b) the bias-uncorrected ground deformation velocity differences were mapped using the SB networks at 6 and 148 days. (c) Map of the bias-corrected ground deformation velocity differences between the SB networks at 6 and 148 days. Only pixels characterized by temporal coherence larger than 0.7 are depicted.

the LOS-projected mean displacement map of the area obtained by applying the SBAS technique to a sequence of 226 S-1 SAR images collected from January 2014 to December 2022.

No significant displacement signals were observed over Venice; however, within the low-lying lagoon

terrain, some spot regions are affected by substantial subsidence, which, associated with sea level rise, can severely impact the area.

Furthermore, CD analyses were carried out. We considered the flood event on 12 November 2019 and used pre- and post-flood SAR images acquired at

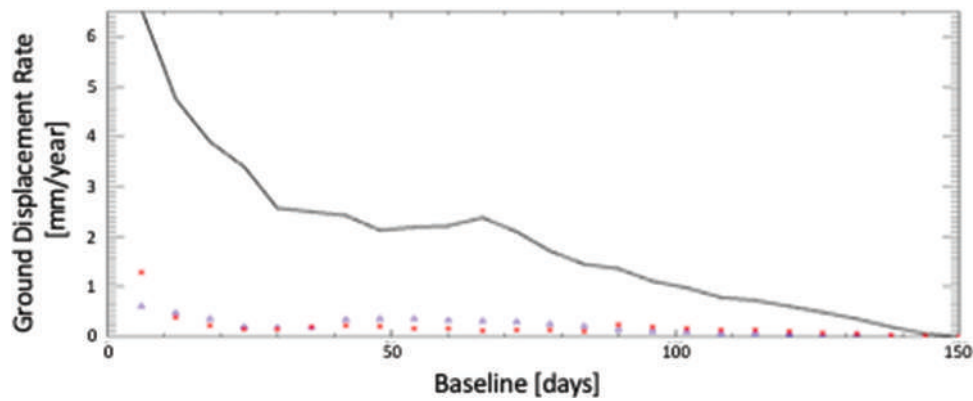


Figure 11. Average absolute values of mean biased ground displacement computed by differencing ground deformation velocities using SB networks at given temporal baseline thresholds and those achieved considering a maximum temporal baseline of 148 days. Black continuous line, no corrections applied; red stars, the time-invariant correction applied; and blue triangles, the time-variant correction applied. Pixels with temporal coherence values greater than 0.7 have been considered.

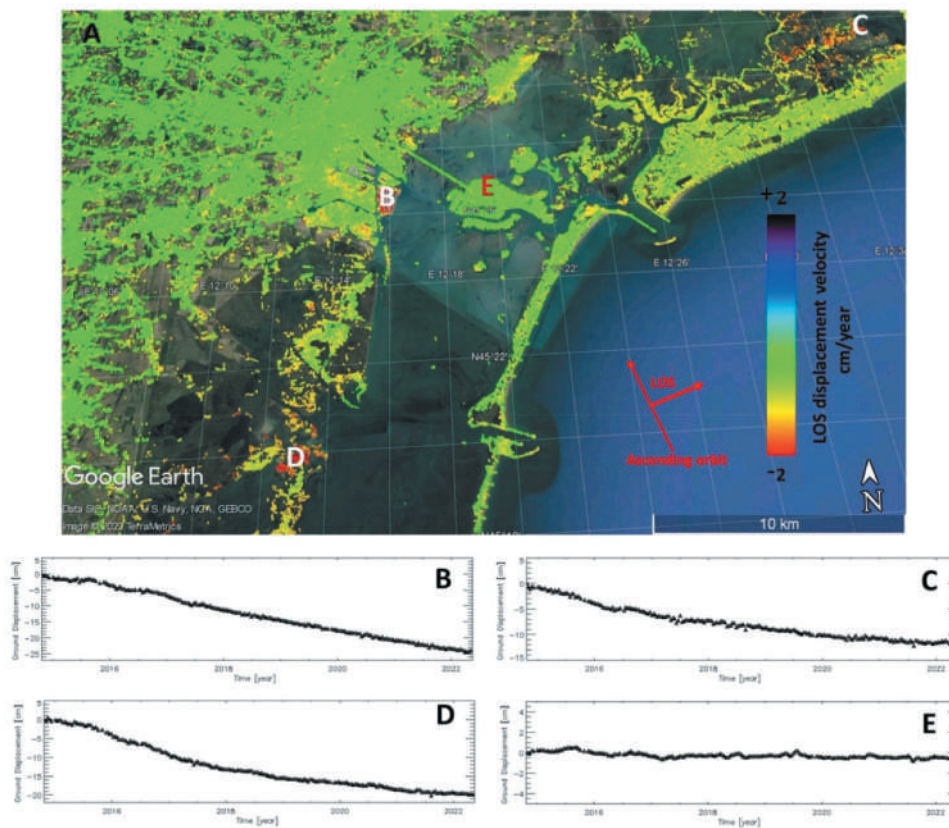


Figure 12. Venice lagoon, Italy: 2014–2022 mean deformation velocity map (A). Time series of deformation related to measure points (B–E).

VV and VH polarizations. Temporal multi-looked sigma-nought (σ_0) maps and Coherence Change Indexes (CCI) were used to feed the proposed AI-based algorithm to perform CD analyses over Venice. CD indices comprise i) the pre-post sigma-nought difference ($\Delta\sigma_0$), ii) the pre-post coherence ratio, and iii) the normalized coherence difference. Specifically, we selected a time series of SAR acquisitions, with temporal baselines of ± 6 , ± 12 , and ± 18 days, before (6 November, 31 and 25 October), during

(12 November), and after (18, 24 and 30 November) the flood event. Every SAR image of the time series was independently post-processed by applying a despeckling noise filtering algorithm (Zhu, Wen, and Zhang 2013). The SLC images were co-registered using Enhanced Spectral Diversity (ESD) (Amin 1993; Mastro and Pepe 2021; Scheiber and Moreira 2000) considering the 12 November 2019 acquisition as a reference: $\Delta\sigma_0$ CDIs were also computed with respect to the same image. Readers are referred to

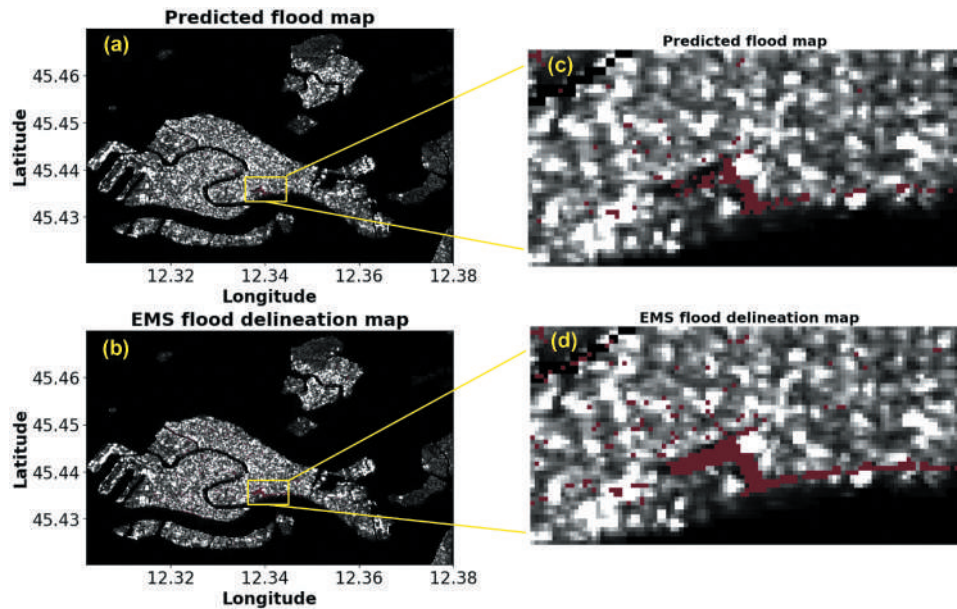


Figure 13. (a) Predicted change masks derived from the proposed methodology and (b) from the Copernicus EMS of Venice city area. Both masks are colored in red and superimposed over SAR amplitude images. Yellow boxes are located in the Piazza San Marco area and zoomed in panels (c) and (d).

(Mastro et al. 2022) for extensive details on determining the exploited CDIs and their statistical inference.

The flooded regions detected using the proposed method are compared with the delineation maps produced by the Copernicus EMS (Figure 13). The Copernicus EMS generates its delineations by visually interpreting satellite images after the flood event. By focusing on the zoom views in Figure 13(c,d), which show the world-famous historical Piazza San Marco of Venice, we can observe the remarkable effectiveness of the proposed methodology in precisely identifying the flooded pixels. A comprehensive evaluation of the CD performances of the proposed method has been extensively documented in Mastro et al. (2022). The results consistently demonstrated an average F1 score (Dalianis 2018; Tharwat 2020) exceeding 0.90, proving the methodology's effectiveness in accurately identifying significant changes while minimizing false alarms.

3.4. SAR data for studying marine environments

This section shows results obtained using the DCA technique (see Section 2.2) to point out the relevance of such a SAR-related research field for supporting coastal environment protection and reducing coastal disaster risks.

The case study presented here is situated in southern Italy, including the Gulf of Naples with the Ischia, Procida and Capri Islands and part of the Gulf of Salerno. The choice of this coastal study area is related to its peculiarities: a) oceanographic and morphological characteristics, b) a highly urbanized coastline, and c) intense

maritime traffic. These elements have increased the interest in the analysis carried out, as they can contribute to the study of the sea state and could provide interesting insights to support Blue Economy strategies.

A data archive composed of 47 ENVISAT-ASAR images acquired over ascending orbit in the 2002–2010 period has been used for the analysis.

Several images of this area of interest have shown the presence of an amplitude signature likely associated with currents. Some of the most exciting results relating to the estimation of the surface current were presented in Jackson et al. (2015) and in Zamparelli et al. (2016); furthermore, in Zamparelli et al. (2020) and in Zamparelli et al. (2020) is presented a methodology which allows quantifying the influence of the wind contribution in the surface currents derived from the DCA.

Here, the sea surface estimation results obtained for the acquisition of 22 September 2010 are reported (Figure 14). In panel A (the σ^0 image), a pattern is discernible in the coastal region north of the Gulf of Naples. The estimated Doppler Anomaly map converted to the sea surface (LOS component) velocity (v_r) is shown in panel B. Redshifts of the estimated sea surface velocity component indicate the motion toward the radar antenna. In contrast, blueshifts indicate the movement away from the radar antenna, being the sea surface velocity direction orthogonal to the flight path. Here, in the same area of panel A, a red pattern corresponding to a surface current approaching the sensor can be observed. Also, another red pattern in the southernmost region, always corresponding to surface currents approaching the sensor, is visible.

22/09/2010

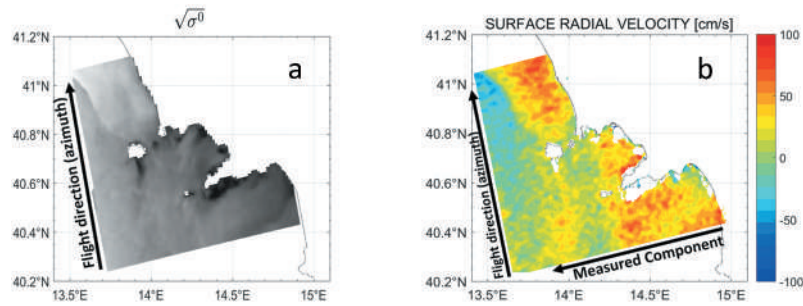


Figure 14. Results related to the ascending ENVISAT acquisition of 22/09/2010. Panel a represents the σ_0 , while panel B is the estimated Doppler Anomaly map of the marine area converted into the sea surface velocity LOS component (v_r).

It is worth noting that the variability of the estimated radial component of the sea surface velocity takes values of ± 100 cm/s (Zamparelli et al. 2020).

From a comparison of the amplitude images and the v_r map (panel B), we can appreciate an excellent correlation between the features of sharp change of surface displacement and signature likely associated with currents in the radar backscatter. In particular, the intense zonal gradient northern to the Gulf indicates a possible switch in the direction of the current water fields. This can be related to the passage from the wind-driven coastal water circulation to the open ocean thermohaline flow.

We must point out, however, that the DCA is the result of many factors, i.e. the sea current, the wind field and the sea waves, besides the wave-current and the wave-wave interactions (Chapron 2005; Johannessen et al. 2008). In the last decades, many efforts have been made to estimate the main parameters of the sea state to separate each of them. Today, SAR-based applications are relatively established for wind derivation at the ocean surface (Alpers et al. 2013; Mouche et al. 2012). Furthermore, preliminary results obtained in the Mediterranean Sea related to the wind field estimation through the use of SAR to evaluate wind influence on the DCA map are presented in Virginia Zamparelli et al. (2020), Signell et al. (2010) and Virginia Zamparelli et al. (2023).

Lastly, to show how the DCA technique is increasing scientific interest, we want to mention a recent study (Amadori et al. 2021), which presents the feasibility of extracting the surface velocity from DCA in lakes. The test case considered is Lake Garda, a large and deep lake in northern Italy. This is a challenging and innovative issue, as SAR images provide synoptic coverage, fine spatial detail, and repeated regular sampling, unlike the data obtained with standard instruments used in lakes.

4. Discussion

Coastal regions are worldwide experiencing unsustainable anthropic pressures, becoming extremely

vulnerable to natural and human-made hazards. Conventional and cutting-edge methods relying on active SAR remote sensing prove to be a powerful tool for mapping and monitoring surface changes affecting coastal/marine environments, with relevant implications for designing and implementing environmental protection strategies.

The availability of long sequences of SAR data collected by the recently launched constellation, such as the Sentinel-1 EU Copernicus satellites, opens to comprehensive studies allowing for a deeper understanding of the long-term Earth surface processes but also poses the challenge of performing more efficient SAR data processing. Moreover, the reduced repetition time of SAR observations (i.e. of 1 week or less) permits us to recover in sequences of short baseline interferogram tiny signals, which are usually not relevant in interferograms with temporal baselines longer than 1 month or so, allowing us to have new independent measurements on the state and changes of vegetation cover (see Section 3.2), such as the water content and soil moisture.

The possibility to complement information derived from both the amplitude and phase of SAR data by exploiting methods based on artificial intelligence has opened the way for the development of new hybrid approaches, such as those shown in Section 3.3, allowing to improve the analyses and go toward a pre-operational use of SAR technologies in disaster risk reduction.

5. Conclusion

This work provides readers with the results of a series of heterogeneous experiments based on exploiting consolidated and novel SAR technologies over several coastal and marine test sites worldwide, pointing out the significant methodological and application-oriented developments resulting from fruitful cooperation among European and Chinese partners. The shown activities represent the starting point of further analyses that will be performed in the following years, primarily aimed at the follows:

- (i) Developing innovative methods for retrieving localized signals in sets of multi-look SAR interferograms and correcting time-correlated phase unwrapping mistakes by enhancing the potential of the methods described in Section 3.2 for the estimation/compensation of phase bias signals.
- (ii) Developing and applying AI methodologies (De et al. 2017; Liu and Lathrop 2002; Mastro et al. 2022) to extract helpful information on the state of the Earth's surface to assess disaster conditions and mitigate the associated risk in coastal areas.
- (iii) Enhancing the exploitation of SAR data for observing marine, coastal-maritime and riverine systems, emphasizing new SAR data collected at various operational wavelengths.
- (iv) Evaluating the potential of the recently launched Spanish PAZ satellite operating in X-band for various applications and EO studies. PAZ data are being tested over the Konya basin, a strategic area in Central Turkey, facing several environmental problems and geohazards due to human activities and geological settings (Caló et al. 2017).

Disclosure statement

No potential conflict of interest was reported by the author(s).

Funding

This work was supported by the DRAGON 5 ESA-MOST GREENISH project [grant number 58351].

Notes on contributors

Qing Zhao is an Associate Professor of East China Normal University, China. Her research interests are about remote sensing applications and Earth Observation, with a particular emphasis on the study of coastal and riverine estuaries environments.

Antonio Pepe (Senior Member, IEEE) received the Laurea degree in electronic engineering and the Ph.D. degree in electronic and telecommunication engineering from the University of Naples Federico II, Naples, Italy, in 2000 and 2007, respectively. After graduation, in 2001, he joined the Istituto per il Rilevamento Elettromagnetico dell'Ambiente (IREA), Italian National Research Council (CNR), Naples, where he currently holds a permanent position of a Research Director. His main research interests include the development of advanced differential synthetic aperture radar interferometry (DInSAR) algorithms for the monitoring of surface deformation phenomena.

Virginia Zamparelli received her Master's degree in Telecommunications Engineering in 2009 at the Federico II University of Naples and the PhD degree in Electrical and Information Engineering at the University of Cassino and Southern Lazio in 2014. In 2010, she participated in the

establishment of Remocean srl, a spin-off of CNR, a marine and coastal monitoring company. In 2013, she was a visiting student at the Polytechnic University of Catalonia Barcelona, Spain. Since 2010 she has been working at National Research Council (CNR) of Italy, Institute of Electromagnetic Sensing of Environment in Napoli, first as Research Fellow and then as permanent Researcher. Her interests concern the development and application of SAR algorithms for the study of marine environment with satellite and airborne platforms.

Pietro Mastro (Member IEEE) Received the Ph.D. degree in Engineering for Innovation and Sustainable Development with the University of Basilicata, Potenza, Italy in 2023. Received the M.S. degree (summa cum laude) in Computer Engineering and Information Technology from the University of Basilicata, Potenza, Italy in 2019. In 2022, he joined the Institute for Electromagnetic Sensing of the Environment (IREA), Naples, as a Research Assistant. His research includes the application of Machine Learning (ML) algorithms that synergistically utilize SAR and optical measurements to study the environment, land processes, and surface parameters.

Francesco Falabella (Member, IEEE) Received the Ph.D. degree in Engineering for Innovation and Sustainable Development, the B.Sc. degree in computer science and information technology and the M.Sc. degree (cum laude) in information technology and telecommunications engineering from the University of Basilicata, Potenza, Italy, in 2023, 2016 and 2019, respectively. In 2022, he joined the Institute for Electromagnetic Sensing of the Environment (IREA), Naples, Italy, as Research Assistant. In 2019, he joined the Institute for Electromagnetic Sensing of the Environment (IREA), Naples, Italy, and the Institute of Methodologies for Environmental Analysis (IMAA), National Research Council (CNR) of Italy, Tito, Italy, as a Research Associate. His research interests include synthetic aperture radar (SAR) data processing, ground-based SAR interferometry, advanced multitemporal interferometric SAR (InSAR) techniques, and environmental remote sensing and applications.

Saygin Abdikan received his MSc. and PhD. in Geomatics Engineering, Remote Sensing and GIS program from Yildiz Technical University, Istanbul, Turkey in 2007 and 2013, respectively. He was awarded Huygens Scholarship by Dutch Government and studied for two years from 2009 to 2011 in the radar group of the Geoscience and Remote Sensing Department, Delft University of Technology, Delft, the Netherlands. Currently, he is working as an Associate Prof. Dr. at Hacettepe University, Ankara, Turkey. His main research interests are about SAR remote sensing, SAR interferometry, deformation monitoring, and information extraction from SAR and optical images.

Cağlar Bayik is a research assistant at Zonguldak Bülent Ecevit University, Turkey. He received the B.Sc., M.Sc., Ph.D. degrees in geomatics engineering from the Zonguldak Bülent Ecevit University, Zonguldak, Turkey, in 2010, 2012, and 2018, respectively. His research interests include SAR remote sensing, SAR interferometry, deformation monitoring, and information extraction from SAR and optical images.

Fusun Balik Sanli received her MSc degree in ITC, The Netherlands, in 2000. She received a Ph.D. in Geomatics Engineering, Remote Sensing, and GIS program from YTU,

Istanbul, Turkey, in 2004. Currently, she is working as an academic staff in the Photogrammetry Division of the Geomatic Engineering Department, YTU. Her research includes optical and radar remote sensing, image fusion, information extraction from SAR and optical images.

Mustafa Üstüner (Member IEEE) received the M.Sc and Ph.D. degree in Geomatic Engineering from Yildiz Technical University, Türkiye in 2014 and 2020, respectively. He is currently working as an assistant professor for the Department of Geomatic Engineering in Artvin Çoruh University, Türkiye. He has been voluntarily working for the IEEE Geoscience and Remote Sensing Society as the Conference & Symposia Liaison. His research includes Applied Machine Learning, PolSAR data analysis, dimensionality reduction and classification of hyperspectral images.

Nevin Betül Avşar is a Professor at the Department of Geomatic Engineering, Artvin Çoruh University, 08100 Artvin, Turkey. Her interests are about the study of sea level changes in Marmara and Black Sea areas.

Jingjing Wang is working at East China Normal University in the field of remote sensing technology.

Peng Chen is working at East China Normal University in the field of remote sensing technology.

Zhengjie Li is working at East China Normal University in the field of remote sensing technology.



Adam T. Devlin is a physical oceanographer who analyzes the fluctuations in tides and sea level on a global and regional level, with a special interest in the dynamics of the Western Pacific Ocean. He also studies the patterns of water level and meteorological changes using historical records and modern satellite data to better predict future flood scenarios and impacts on coastal populations and ecosystems. Dr. Devlin holds a Ph.D. in Applied Physics from Portland State University, an MS in Applied Physics from Appalachian State University, and a BS in Physics from the University of Oregon. He worked at the Chinese University of Hong Kong from 2016 to 2019. Dr. Devlin joined the School of Geography and Environment, Jiangxi Normal University as a distinguished research professor in May 2019. Currently, he works at the University of Hawaii, U.S.

Fabiana Calò received her Master's degree in Environmental Engineering from Politecnico di Bari (2004) and a PhD in Analysis of Environmental Systems at University of Napoli Federico II (2010). She has been Visiting Scientist at Canada Centre for Remote Sensing, Ottawa (2008) and Yildiz Technical University, Istanbul (2014–2015). Since 2010 she works at National Research Council (CNR) of Italy, Institute of Electromagnetic Sensing of Environment in Napoli, first as Post-Doc fellow and then as permanent Researcher. Her research interests mainly focus on the study of natural and man-made hazards, and on the natural resources protection by integrating ground-based and Earth Observation data analyses.

ORCID

Qing Zhao  <http://orcid.org/0000-0003-3433-9435>
 Antonio Pepe  <http://orcid.org/0000-0002-7843-3565>
 Virginia Zamparelli  <http://orcid.org/0000-0003-2829-0903>

Pietro Mastro  <http://orcid.org/0000-0002-3299-3567>
 Francesco Falabella  <http://orcid.org/0000-0002-3698-908X>

Saygin Abdikan  <http://orcid.org/0000-0002-3310-352X>
 Caglar Bayik  <http://orcid.org/0000-0001-6606-3272>
 Fusun Balik Sanli  <http://orcid.org/0000-0003-1243-8299>
 Mustafa Ustuner  <http://orcid.org/0000-0003-0553-2682>
 Nevin Betül Avşar  <http://orcid.org/0000-0001-7402-6201>
 Adam T. Devlin  <http://orcid.org/0000-0002-4334-0828>
 Fabiana Calò  <http://orcid.org/0000-0002-0174-5894>

Data availability statement

The SRTM DEM was freely downloaded from the USGS Earth Explorer site. The TanDEM-X was obtained from German Aerospace Center (DLR) data website. Sentinel-1 data were freely derived from the following resources available in the public domain: [<https://scihub.copernicus.eu/>]. ASAR ENVISAT data was freely derived from the following resources available in the public domain: [<https://eocat.esa.int/sec/#data-services-area>]. Due to commercial restrictions, TanDEM-X, RADARSAT-2 and PAZ data sharing are not open.

References

- Alpers, W., A. Mouche, J. Horstmann, A. Ivanov, and V. Barabanov. 2013. "Test of an Advanced Algorithm to Retrieve Complex Wind Fields Over the Black Sea from Envisat SAR Images." In *2013 IEEE International Geoscience and Remote Sensing Symposium (IGARSS)*. Melbourne, July 21–26.
- Amadori, M., V. Zamparelli, G. De Carolis, G. Fornaro, M. Toffolon, M. Bresciani, C. Giardino, and F. De Santi. 2021. "Monitoring Lakes Surface Water Velocity with SAR: A Feasibility Study on Lake Garda, Italy." *Remote Sensing* 13 (12): 2293. <https://doi.org/10.3390/rs13122293>.
- Amin, M. G. 1993. "Introducing the Spectral Diversity." *IEEE Transactions on Signal Processing* 41 (1): 185–193. <https://doi.org/10.1109/TSP.1993.193137>.
- Ansari, H., F. De Zan, and A. Parizzi. 2021. "Study of Systematic Bias in Measuring Surface Deformation with SAR Interferometry." *IEEE Transactions on Geoscience and Remote Sensing* 59 (2): 1285–1301. <https://doi.org/10.1109/TGRS.2020.3003421>.
- Barber, J. 2015. "A Generalized Likelihood Ratio Test for Coherent Change Detection in Polarimetric SAR." *IEEE Geoscience and Remote Sensing Letters* 12 (9): 1873–1877. <https://doi.org/10.1109/LGRS.2015.2433134>.
- Bates, P. D., and A. P. J. De Roo. 2000. "A Simple Raster-Based Model for Flood Inundation Simulation." *Journal of Hydrology* 236 (1–2): 54–77. [https://doi.org/10.1016/S0022-1694\(00\)00278-X](https://doi.org/10.1016/S0022-1694(00)00278-X).
- Bazi, Y., L. Bruzzone, and F. Melgani. 2006. "Automatic Identification of the Number and Values of Decision Thresholds in the Log-Ratio Image for Change Detection in SAR Images." *IEEE Geoscience and Remote Sensing Letters* 3 (3): 349–353. <https://doi.org/10.1109/LGRS.2006.869973>.
- Belgiu, M., and L. Drăguț. 2016. "Random Forest in Remote Sensing: A Review of Applications and Future Directions." *ISPRS Journal of Photogrammetry and Remote Sensing* 114 (April): 24–31. <https://doi.org/10.1016/j.isprsjprs.2016.01.011>.

- Berardino, P., G. Fornaro, R. Lanari, and E. Sansosti. 2002. "A New Algorithm for Surface Deformation Monitoring Based on Small Baseline Differential SAR Interferograms." *IEEE Transactions on Geoscience and Remote Sensing* 40 (11): 2375–2383. <https://doi.org/10.1109/TGRS.2002.803792>.
- Breiman, L. 2001. "Random Forests." *Machine Learning* 45 (1): 5–32. <https://doi.org/10.1023/A:1010933404324>.
- Bresciani, M., N. Ghirardi, G. Fornaro, V. Zamparelli, F. De Santi, G. De Carolis, D. Tapete, M. Palandri, and C. Giardino. 2021. "Combined Use of Optical and SAR Images for Mapping Coastal Erosion Risk." In *2021 IEEE International Geoscience and Remote Sensing Symposium (IGARSS)*. Brussels, July 12–16.
- Calò, F., S. Abdikan, T. Görüm, A. Pepe, H. Kiliç, and F. B. Şanlı. 2015. "The Space-Borne SBAS-DInSAR Technique as a Supporting Tool for Sustainable Urban Policies: The Case of Istanbul Megacity, Turkey." *Remote Sensing* 7 (12): 16519–16536. <https://doi.org/10.3390/rs71215842>.
- Caló, F., D. Notti, J. P. Galve, S. Abdikan, T. Görüm, A. Pepe, and F. B. Şanlı. 2017. "DInSAR-Based Detection of Land Subsidence and Correlation with Groundwater Depletion in Konya Plain, Turkey." *Remote Sensing* 9 (1): 83. <https://doi.org/10.3390/rs9010083>.
- Chapron, B. 2005. "Direct Measurements of Ocean Surface Velocity from Space: Interpretation and Validation." *Journal of Geophysical Research* 110 (C7): C07008. <https://doi.org/10.1029/2004JC002809>.
- Cianelli, D., M. Uttieri, B. Buonocore, P. Falco, G. Zambardino, and E. Zambianchi. 2012. "Dynamics of a Very Special Mediterranean Coastal Area: The Gulf of Naples." In *Mediterranean Ecosystems: Dynamics, Management and Conservation*, edited by G. S. Williams, 129–150. New York: Nova.
- Dalianis, H. 2018. "Evaluation Metrics and Evaluation." In *Clinical Text Mining: Secondary Use of Electronic Patient Records*, edited by H. Dalianis, 45–53. Kista, Sweden: Springer International Publishing. https://doi.org/10.1007/978-3-319-78503-5_6.
- De, S., D. Pirrone, F. Bovolo, L. Bruzzone, and A. Bhattacharya. 2017. "A Novel Change Detection Framework Based on Deep Learning for the Analysis of Multi-Temporal Polarimetric SAR Images." In *2017 IEEE International Geoscience and Remote Sensing Symposium (IGARSS)*. Fort Worth, July 23–28.
- Falabella, F., and A. Pepe. 2022a. "Non-Closure Phase of Multi-Look InSAR Triplets: A Novel Phase Bias Mitigation Method." In *2022 IEEE International Geoscience and Remote Sensing Symposium (IGARSS)*. Kuala Lumpur, July 17–22.
- Falabella, F., and A. Pepe. 2022b. "On the Phase Nonclosure of Multilook SAR Interferogram Triplets." *IEEE Transactions on Geoscience and Remote Sensing* 60:1–17. <https://doi.org/10.1109/TGRS.2022.3216083>.
- Ferretti, A., A. Fumagalli, F. Novali, C. Prati, F. Rocca, and A. Rucci. 2011. "A New Algorithm for Processing Interferometric Data-Stacks: SqueeSar." *IEEE Transactions on Geoscience and Remote Sensing* 49 (9): 3460–3470. <https://doi.org/10.1109/TGRS.2011.2124465>.
- Ferretti, A., C. Prati, and F. Rocca. 2001. "Permanent Scatterers in SAR Interferometry." *IEEE Transactions on Geoscience and Remote Sensing* 39 (1): 8–20. <https://doi.org/10.1109/36.898661>.
- Fiscella, B., A. Giancaspro, F. Nirchio, P. Pavese, and P. Trivero. 2000. "Oil Spill Detection Using Marine SAR Images." *International Journal of Remote Sensing* 21 (18): 3561–3566. <https://doi.org/10.1080/014311600750037589>.
- Global Climate Change. "Sea Level Rise, Extreme Events and Local Ground Subsidence Effects in Coastal and River Delta Regions Through Novel and Integrated Remote Sensing Approaches (GREENISH). S.D." Dragon 5 Cooperation. Consultato gennaio 24, 2023. <https://dragon5.esa.int/projects/global-climate-change-sea-level-rise-extreme-events-and-local-ground-subsidence-effects-in-coastal-and-river-delta-regions-through-novel-and-integrated-remote-sensing-approaches-greenish/>.
- Hooper, A. 2008. "A Multi-Temporal InSAR Method Incorporating Both Persistent Scatterer and Small Baseline Approaches." *Geophysical Research Letters* 35 (16): L16302. <https://doi.org/10.1029/2008GL034654>.
- Jackson, G., G. Fornaro, P. Berardino, C. Esposito, R. Lanari, A. Pauciuolo, D. Reale, V. Zamparelli, and S. Perna. 2015. "Experiments of Sea Surface Currents Estimation with Space and Airborne SAR Systems." In *2015 IEEE International Geoscience and Remote Sensing Symposium (IGARSS)*. Milan, July 26–31.
- Johannessen, J. A., B. Chapron, F. Collard, V. Kudryavtsev, A. Mouche, D. Akimov, and K. F. Dagestad. 2008. "Direct Ocean Surface Velocity Measurements from Space: Improved Quantitative Interpretation of Envisat ASAR Observations." *Geophysical Research Letters* 35 (22): L22608. <https://doi.org/10.1029/2008GL035709>.
- Kennish, M. J., H. W. Paerl, M. J. Kennish, and H. W. Paerl. 2010. *Coastal Lagoons: Critical Habitats of Environmental Change*. Boca Raton, Florida, USA: CRC Press. <https://doi.org/10.1201/EBK1420088304>.
- Kerbaol, V., and F. Collard. 2005. "SAR-Derived Coastal and Marine Applications: From Research to Operational Products." *IEEE Journal of Oceanic Engineering* 30 (3): 472–486. <https://doi.org/10.1109/JOE.2005.857505>.
- Klemas, V. 2015. "Remote Sensing of Floods and Flood-Prone Areas: An Overview." *Journal of Coastal Research* 314 (July): 1005–1013. <https://doi.org/10.2112/JCOASTRES-D-14-00160.1>.
- Kratzer, S., K. Alikas, T. Harvey, J. M. Beltrán-Abaunza, E. Morozov, S. Ben Mustapha, and S. Lavender. 2016. *Multitemporal Remote Sensing of Coastal Waters: Remote Sensing and Digital Image Processing*. Stockholm, Sweden: Springer International Publishing. https://doi.org/10.1007/978-3-319-47037-5_19.
- Laignel, B., S. Vignudelli, R. Almar, M. Becker, A. Bentamy, J. Benveniste, F. Birol, et al. 2023. "Observation of the Coastal Areas, Estuaries and Deltas from Space." *Surveys in Geophysics*. <https://doi.org/10.1007/s10712-022-09757-6>.
- Liu, X., and R. G. Lathrop. 2002. "Urban Change Detection Based on an Artificial Neural Network." *International Journal of Remote Sensing* 23 (12): 2513–2518. <https://doi.org/10.1080/01431160110097240>.
- Madsen, S. N. 1989. "Estimating the Doppler Centroid of SAR Data." *IEEE Transactions on Aerospace and Electronic Systems* 25 (2): 134–140. <https://doi.org/10.1109/7.18675>.
- Maghsoudi, Y., A. J. Hooper, T. J. Wright, M. Lazecky, and H. Ansari. 2022. "Characterizing and Correcting Phase Biases in Short-Term, Multilooked Interferograms." *Remote Sensing of Environment* 275 (June): 113022. <https://doi.org/10.1016/j.rse.2022.113022>.
- Mastro, P., G. Masiello, C. Serio, and A. Pepe. 2022. "Change Detection Techniques with Synthetic Aperture Radar Images: Experiments with Random Forests and

- Sentinel-1 Observations.” *Remote Sensing* 14 (14): 3323. <https://doi.org/10.3390/rs14143323>.
- Mastro, P., and A. Pepe. 2021. “The Triplet Network Enhanced Spectral Diversity (T-NESD) Method for the Correction of TOPS Data Co-Registration Errors for Non-Stationary Scenes.” In *2021 IEEE International Geoscience and Remote Sensing Symposium (IGARSS)*. Brussels, July 12–16.
- Mouche, A. A., F. Collard, B. Chapron, K. F. Dagestad, G. Guitton, J. A. Johannessen, V. Kerbaol, and M. W. Hansen. 2012. “On the Use of Doppler Shift for Sea Surface Wind Retrieval from SAR.” *IEEE Transactions on Geoscience and Remote Sensing* 50 (7): 2901–2909. <https://doi.org/10.1109/TGRS.2011.2174998>.
- Pepe, A. 2021. “Multi-Temporal Small Baseline Interferometric SAR Algorithms: Error Budget and Theoretical Performance.” *Remote Sensing* 13 (4): 557. <https://doi.org/10.3390/rs13040557>.
- Pepe, A., and F. Calò. 2017. “A Review of Interferometric Synthetic Aperture RADAR (InSar) Multi-Track Approaches for the Retrieval of Earth’s Surface Displacements.” *Applied Sciences* 7 (12): 1264. <https://doi.org/10.3390/app7121264>.
- Pepe, A., and R. Lanari. 2006. “On the Extension of the Minimum Cost Flow Algorithm for Phase Unwrapping of Multitemporal Differential SAR Interferograms.” *IEEE Transactions on Geoscience and Remote Sensing* 44 (9): 2374–2383. <https://doi.org/10.1109/TGRS.2006.873207>.
- Pepe, A., and P. Mastro. 2017. “On the Use of Directional Statistics for the Adaptive Spatial Multi-Looking of Sequences of Differential SAR Interferograms.” In *2017 IEEE International Geoscience and Remote Sensing Symposium (IGARSS)*. Fort Worth, July 23–28.
- Pepe, A., P. Mastro, and C. E. Jones. 2021. “Adaptive Multilooking of Multitemporal Differential SAR Interferometric Data Stack Using Directional Statistics.” *IEEE Transactions on Geoscience and Remote Sensing* 59 (8): 6706–6721. <https://doi.org/10.1109/TGRS.2020.3030003>.
- Pepe, A., G. Solaro, F. Calò, and C. Dema. 2016. “A Minimum Acceleration Approach for the Retrieval of Multiplatform InSar Deformation Time Series.” *IEEE Journal of Selected Topics in Applied Earth Observations and Remote Sensing* 9 (8): 3883–3898. <https://doi.org/10.1109/JSTARS.2016.2577878>.
- Pepe, A., Y. Yang, M. Manzo, and R. Lanari. 2015. “Improved EMCF-SBAS Processing Chain Based on Advanced Techniques for the Noise-Filtering and Selection of Small Baseline Multi-Look DInSar Interferograms.” *IEEE Transactions on Geoscience and Remote Sensing* 53 (8): 4394–4417. <https://doi.org/10.1109/TGRS.2015.2396875>.
- Qin, T., K. L. Wu, and D. B. Xiu. 2019. “Data Driven Governing Equations Approximation Using Deep Neural Networks.” *Journal of Computational Physics* 395 (October): 620–635. <https://doi.org/10.1016/j.jcp.2019.06.042>.
- Romeiser, R., H. Runge, S. Suchandt, R. Kahle, C. Rossi, and P. S. Bell. 2014. “Quality Assessment of Surface Current Fields from TerraSAR-X and TanDEM-X Along-Track Interferometry and Doppler Centroid Analysis.” *IEEE Transactions on Geoscience and Remote Sensing* 52 (5): 2759–2772. <https://doi.org/10.1109/TGRS.2013.2265659>.
- Rosen, P. A., S. Hensley, E. Gurrola, F. Rogez, S. Chan, J. Martin, and E. Rodriguez. 2001. “SRTM C-Band Topographic Data: Quality Assessments and Calibration Activities.” In *2001 IEEE International Geoscience and Remote Sensing Symposium (IGARSS)*. Sydney, July 9–13.
- Scheiber, R., and A. Moreira. 2000. “Coregistration of Interferometric SAR Images Using Spectral Diversity.” *IEEE Transactions on Geoscience and Remote Sensing* 38 (5): 2179–2191. <https://doi.org/10.1109/36.868876>.
- Shirzaei, M. 2015. “A Seamless Multitrack Multitemporal InSar Algorithm.” *Geochemistry, Geophysics, Geosystems* 16 (5): 1656–1669. <https://doi.org/10.1002/2015GC005759>.
- Signell, R. P., J. Chiggiato, J. Horstmann, J. D. Doyle, J. Pullen, and F. Askari. 2010. “High-Resolution Mapping of Bora Winds in the Northern Adriatic Sea Using Synthetic Aperture Radar.” *Journal of Geophysical Research-Oceans* 115 (C4): C04020. <https://doi.org/10.1029/2009JC005524>.
- Tang, M. C., Q. Zhao, A. Pepe, A. T. Devlin, F. Falabella, C. F. Yao, and Z. J. Li. 2022. “Changes of Chinese Coastal Regions Induced by Land Reclamation as Revealed Through TanDEM-X DEM and InSar Analyses.” *Remote Sensing* 14 (3): 637. <https://doi.org/10.3390/rs14030637>.
- Teatini, P., L. Tosi, T. Strozzi, L. Carbognin, U. Wegmüller, and F. Rizzetto. 2005. “Mapping Regional Land Displacements in the Venice Coastland by an Integrated Monitoring System.” *Remote Sensing of Environment* 98 (4): 403–413. <https://doi.org/10.1016/j.rse.2005.08.002>.
- Tello, M., C. Lopez-Martinez, and J. J. Mallorqui. 2005. “A Novel Algorithm for Ship Detection in SAR Imagery Based on the Wavelet Transform.” *IEEE Geoscience and Remote Sensing Letters* 2 (2): 201–205. <https://doi.org/10.1109/LGRS.2005.845033>.
- Tharwat, A. 2020. “Classification Assessment Methods.” *Applied Computing & Informatics* 17 (1): 168–192. <https://doi.org/10.1016/j.aci.2018.08.003>.
- Trivero, P., M. Adamo, W. Biamino, M. Borasi, M. Cavignerio, G. De Carolis, L. Di Matteo, F. Fontebasso, F. Nirchio, and F. Tataranni. 2016. “Automatic Oil Slick Detection from SAR Images: Results and Improvements in the Framework of the PRIMI Pilot Project.” *Deep Sea Research Part II: Topical Studies in Oceanography* 133 (novembre): 146–158. <https://doi.org/10.1016/j.dsr2.2016.03.003>.
- Zakhvatkina, N., V. Smirnov, and I. Bychkova. 2019. “Satellite SAR Data-Based Sea Ice Classification: An Overview.” *Geosciences* 9 (4): 152. <https://doi.org/10.3390/geosciences9040152>.
- Zamparelli, V., F. De Santi, A. Cucco, S. Zecchetto, G. De Carolis, and G. Fornaro. 2020. “Surface Currents Derived from SAR Doppler Processing: An Analysis Over the Naples Coastal Region in South Italy.” *Journal of Marine Science and Engineering* 8 (3): 203. <https://doi.org/10.3390/jmse8030203>.
- Zamparelli, V., F. De Santi, G. De Carolis, and G. Fornaro. 2020. “On the Analysis of SAR Derived Wind and Sea Surface Currents.” In *2020 IEEE International Geoscience and Remote Sensing Symposium (IGARSS)*. Hawaii, September 26 - October 2.
- Zamparelli, V., F. De Santi, G. De Carolis, and G. Fornaro. 2023. “SAR Based Sea Surface Complex Wind Fields Estimation: An Analysis Over the Northern Adriatic Sea.” *Remote Sensing* 15 (8): 2074. <https://doi.org/10.3390/rs15082074>.
- Zamparelli, V., G. Jackson, A. Cucco, G. Fornaro, and S. Zecchetto. 2016. “SAR Based Sea Current Estimation in the Naples Coastal Area.” In *2016 IEEE International Geoscience and Remote Sensing Symposium (IGARSS)*, Beijing, July 10–15.

- Zhao, Q., J. Y. Pan, A. T. Devlin, M. C. Tang, C. F. Yao, V. Zamparelli, F. Falabella, and A. Pepe. 2022. "On the Exploitation of Remote Sensing Technologies for the Monitoring of Coastal and River Delta Regions." *Remote Sensing* 14 (10): 2384. <https://doi.org/10.3390/rs14102384>.
- Zheng, Y. J., H. Fattahi, P. Agram, M. Simons, and P. Rosen. 2022. "On Closure Phase and Systematic Bias in Multilooked SAR Interferometry." *IEEE Transactions on Geoscience and Remote Sensing* 60:1–11. <https://doi.org/10.1109/TGRS.2022.3225843>.
- Zhu, J. L., J. G. Wen, and Y. F. Zhang. 2013. "A New Algorithm for SAR Image Despeckling Using an Enhanced Lee Filter and Median Filter." In *2013 6th International Congress on Image and Signal Processing (CISP)*. 224–228. Hangzhou, China: IEEE.